# Process-based modeling of nitrous oxide emissions from wheat-cropped soils at the sub-regional scale

Benoit Gabrielle, Patricia Laville, Odile Duval, Bernard Nicoullaud, Jean-Claude Germon, Catherine Hénault

# Process-based modeling of nitrous oxide emissions from wheat-cropped soils at the sub-regional scale

B. Gabrielle, P. Laville

INRA, INA P-G, Unité Mixte de Recherche Environnement et Grandes Cultures, Thiverval-Grignon, France

O. Duval, B. Nicoullaud

INRA, Unité de Recherche de Science du Sol, Olivet, France

J. C. Germon, C. Hénault

INRA, U. Bourgogne, Unité Mixte de Recherche Microbiologie et Géochimie des Sols, Dijon, France

**Abstract.** Arable soils are a large source of nitrous oxide ($N_2O$) emissions, making up half of the biogenic emissions worldwide. Estimating their source strength requires methods capable of capturing the spatial and temporal variability of $N_2O$ emissions, along with the effects of crop management.
Here, we applied a process-based model, CERES, with geo-referenced input data on soils, weather, and land use to map $N_2O$ emissions from wheat-cropped soils in three agriculturally intensive regions in France. Emissions were mostly controlled by soil type and local climate conditions, and only to a minor extent by the doses of fertilizer nitrogen applied. As a result, the direct emission factors calculated at the regional level were much smaller (ranging from 0.0007 to 0.0033 kg kg $N_2O$-N $kg^{-1}$ N) than the value of 0.0125 kg $N_2O$-N $kg^{-1}$ N currently recommended in the IPCC Tier 1 methodology. Regional emissions were far more sensitive to the soil microbiological parameters governing denitrification and its fraction evolved as $N_2O$, soil bulk density, and soil initial inorganic N content. Mitigation measures should therefore target a reduction in the amount of soil inorganic N upon sowing of winter crops, and a decrease of the soil $N_2O$ production potential itself. From a general perspective, taking into account the spatial variability of soils and climate thereby appears necessary to improve the accuracy of national inventories, and to tailor mitigation strategies to regional characteristics.

## 1. Introduction

Emissions from arable soils are a key item in the global nitrous oxide ($N_2O$) budget, making up about half of the terrestrial biogenic emissions [*Mosier et al.*, 1998]. Since agricultural activities are gradually coming into focus in the greenhouse gas (GHG) budget calculations, precise estimates of current $N_2O$ emissions from arable land are being sought, along with possible means of abatement. However, compared to other GHG such as $CO_2$, $N_2O$ fluxes are of small magnitude and highly variable in space and time [*Duxbury and Bouldin*, 1982], being tightly linked to the local climatic sequence and soil properties. In national GHG inventories, the default recommended method is that defined by *IPCC* [1997], currently being overhauled. It relates direct $N_2O$ emissions to the amount of fertilizer N applied based on a fixed emissions factor, thereafter noted $EF_d$. Although this method is relatively easy to implement, by combination with nationwide economic statistics, it ignores the effect of the above-mentioned characteristics. Also, it cannot be used directly to define crop management strategies that would mitigate $N_2O$ emissions, since it does not account for the effect of fertilizer N application (let alone other management practices) on crop growth and yield.
In the last ten years, the prediction of $N_2O$ emissions within process-based agro-ecosystem models has emerged as a promising route to deal with these issues, primarily at the local scale, to single out the effect of crop management practices [*Li et al.*, 2005]. Application on larger spatial scales has also been demonstrated at the regional, country and sub-continental levels [*Mummey et al.*, 1998; *Li et al.*, 2001; *Butterbach-Bahl et al.*, 2004]. However, it is complicated by the lack of adequate input data and the fact that models may not be robust to such upscaling. In terms of spatial resolution, the above examples involved 16 to 400-$km^2$-wide elementary counties or grid squares, implying that models were run on 'average' soils resulting from the combination of the possibly wide range of soil types occurring in the elementary spatial unit considered. Short-range (< 1 km) variability across agricultural fields was therefore likely to be smoothed out in these spatial extrapolations, which precludes a back-tracking of those zones with high emission potentials on which particular measures might be taken to reduce the efflux of $N_2O$. Also, it makes it impossible to compare the elementary cell-averaged flux with local, ground measurements, the level at which these plot-scale models were generally tested [*Butterbach-Bahl et al.*, 2004]. Upscaling to small areas with a much finer grain has also been reported [*Grant and Pattey*, 2003]. The latter authors simulated $N_2O$ emissions in a 12-ha landscape by means of 50 m x 50 m grid squares, and showed micro-relief to be responsible for emission 'hot-spots' accounting for most of the spatial variability in $N_2O$ efflux. They concluded that aggregation of $N_2O$ emissions at higher scales should be based on 'typical landscapes in which surface topography and soil type is accurately represented'. There is therefore a need for process-based inventories at an intermediate resolution between the field (1-100 ha) and county (10-1000 $km^2$) levels, which would explicitly account for heterogeneities between


0886-6236/06/2006GB002686$12.00

individual soil types.

Here, we report results obtained on such a grain for $N_2O$ emissions from wheat-cropped soils, at the sub-regional level. We used a crop model derived from CERES [*Jones and Kiniry*, 1986], which incorporates a module for $N_2O$ emissions [*Gabrielle et al.*, 2006]. The model was run on elementary units (vectorized contours) resulting from the combination of several information layers in three agricultural sub-regions in Central France. The model parameterization procedure was checked against ground measurements of $N_2O$ emissions in three test sites, and its spatial estimates compared to those obtained with the *IPCC* [1997] method. We assessed the sensitivity of the modeled sub-regional estimates to uncertainties in key physical and microbiological parameters, and evaluated their impacts by means of an uncertainty analysis.

## 2. Material and Methods

### 2.1. The CERES-EGC model

CERES-EGC was adapted from the CERES suite of soil-crop models [*Jones and Kiniry*, 1986], with a focus on the simulation of environmental outputs such as nitrate leaching and gaseous emissions of $N_2O$, ammonia and nitrogen oxides [*Gabrielle et al.*, 2006]. CERES-EGC comprises sub-models for the major processes governing the cycles of water, carbon and nitrogen in soil-crop systems. A physical module simulates the transfer of heat, water and nitrate down the soil profile, as well as soil evaporation, plant water uptake and transpiration in relation to climatic demand. A microbiological module simulates the turnover of organic matter in the plow layer, involving both mineralization and immobilization of inorganic N. Lastly, crop net photosynthesis is a linear function of intercepted radiation according to the Monteith approach, with interception depending on leaf area index based on Beer's law of diffusion in turbid media. Crop N uptake is computed through a supply/demand scheme, with soil supply depending on soil nitrate and ammonium concentrations and root length density.

CERES-EGC includes NOE [*Hénault et al.*, 2005], a semi-empirical sub-model simulating the production and reduction of $N_2O$ in agricultural soils through both the denitrification and nitrification pathways. The denitrification component of NOE is based on NEMIS [*Hénault and Germon*, 2000], a model that expresses total denitrification of soil $NO_3^-$ as the product of a potential rate with three unit-less factors related to soil water content, nitrate content, and temperature. The fraction of denitrified nitrate that evolves as $N_2O$ is considered as constant for a given soil type, according to the experimental evidence provided by *Hénault et al.* [2001]. In a similar fashion, nitrification is modeled as a Michaëlis-Menten reaction, with $NH_4^+$ as substrate. The corresponding rate is multiplied by unit-less modifiers related to soil water content and temperature. As for denitrification, a soil-specific proportion of total nitrification evolves as $N_2O$, following the results of *Garrido et al.* [2002]. The two pathways are connected in that nitrification-derived $N_2O$ may be reduced to $N_2$ by denitrification, should the two processes be simultaneously active. Unlike other $N_2O$ emission modules such as NGAS [*Parton et al.*, 2001] or DNDC [*Li et al.*, 2001], NOE does not use the microbial respiration of organic C as a driver for denitrification.

CERES-EGC runs on a daily time step, and computes the various transformation rates of N with the following sequence: nitrification, denitrification, mineralization/immobilization, and crop uptake. This sequence reflects the priority order for possibly competing processes, such as denitrification and crop uptake of nitrate.

### 2.2. Spatial simulations

#### 2.2.1. Information layers

The study area comprised three administrative 'agricultural sub-regions' of the Beauce region, lying approximately 200 km southwest of Paris, France: Beauce Chartraine (74 000 ha), Beauce Dunoise (61 200 ha), and Faux-Perche (48 200 ha). The sub-regions were delineated by French authorities as relatively homogeneous zones from the point of view of physical characteristics (climate, pedogenesis and geological substrate), and agricultural production systems. The majority of soils in Beauce Chartraine are thick clay loams (Haplic Luvisols - *Isambert* [1984]), either permeable upon limestone parent material, or less permeable material developed on a flinty clay substrate. The mean annual rainfall is 600 mm, and mean air temperature is 10.6 °C. Beauce Dunoise comprises mostly thin loamy clay soils (Haplic Calcisols), developed on calcareous layers. Mean annual rainfall is 636 mm, and mean air temperature is 10.8 °C. Lastly, the soils in Faux-Perche are loamy Gleyic Luvisols, developed on a flint clay substrate. Mean annual rainfall is 783 mm, and mean air temperature is 10.3 °C. Farming systems are based on cereal crops in the first two regions, and include some livestock production in Faux-Perche.

Elementary simulation units were defined by overlaying spatial information soil types, climate, land use and crop management available at various geographical or administrative levels. Only a fraction of the sub-regions was simulated, since we had chosen to focus on winter wheat. Wheat is the major arable crop in the area, being grown on 30% to 40% of total arable land. Each sub-region comprised 4 counties, at which level information on land use was available through agricultural census data and farmers declarations for European subsidies. Typical crop management practices for winter wheat were set based on a survey in the three sub-regions. Soils were parameterized based on a 1:250 000 scale soil map, organized into geographical soil map units (SMU) containing a mixture of soil typological units (STU), following the model of the European Union soil map [*King et al.*, 1994]. The soil data base attached with the map comprised geographical information (the shape of the SMUs) and quantitative data for each SMU: the occurrence of particular STUs within the SMU, and various descriptors characterizing the STUs. The SMUs covered between 3 and 19,000 ha, with an average size of 775 ha. Daily weather data were taken for each simulation unit from the closest station available, less than 20 km away from the centroid of the unit.

#### 2.2.2. Soil parameterization

Various methods were combined to estimate the soil parameters of CERES-EGC. Some were readily-available as thematic fields in the soil data base: depth to parent material (down to 2 m), which was used to set the simulation depth; maximum rooting depth (with an upper limit of 1.5 m); the thickness of the various soil horizons along with their particle-size distribution and bulk density. Soil water contents at wilting point and field-capacity were estimated with pedo-transfer functions developed on a collection of *c.* 600 samples, mostly taken from the Paris basin, with contrasting textures [*Bastet et al.*, 1998]. The saturation water content, also required by CERES-EGC as input, was estimated with the pedo-transfer function originally proposed by CERES [*Jones and Kiniry*, 1986]. Topsoil organic matter content was also included based on a nationwide survey [*Arrouays et al.*, 1999], and updated in the course of this study. Surface pH and $CaCO_3$ contents were added to the data base using local references and expertise, and the same went with saturated hydraulic conductivity. The latter was estimated using only three classes centered on the following values: 0.02, 0.08, and 0.3 m $d^{-1}$, respectively.

The $N_2O$ module of CERES-EGC involves a set of 3 microbiological parameters governing the processes of $N_2O$ production and reduction in soils, as detailed in *Hénault et al.* [2005]. They were measured in the laboratory in each test site of the sub-regions, as follows: potential denitrification rates were measured by acetylene blocking of undisturbed soil cores taken from the top 20 cm of soil, saturated with water and incubated with an ample supply of nitrate [*Hénault and Germon*, 2000]; the fraction of denitrified nitrate that evolves as $N_2O$ was determined as the difference between the $N_2O$ production rates of soil cores incubated with and without acetylene [*Hénault et al.*, 2001]; lastly, the fraction of nitrification evolved as $N_2O$ was measured on sieved soil samples incubated with increasing soil moisture content and non-limiting $NH_3$ supply, using the methodology proposed by *Garrido et al.* [2002]. Table 1 lists the parameter values obtained in the three sites.

**Table 1.** Soil microbiological parameters of NOE measured at the three test sites.

| Symbol | Description (Unit) | Parameter value | | |
|---|---|---|---|---|
| | | La Saussaye | Villamblain | Arrou |
| PDR | Potential denitrification rate (kg N $ha^{-1}$ $d^{-1}$) | 15.7 | 16.9 | 9.4 |
| $r_D$ | Fraction of denitrification evolved as $N_2O$(%) | 20 | 20 | 64 |
| $r_N$ | Fraction of nitrification evolved as $N_2O$(%) | 0.06 | 0.06 | 0.06 |

Unfortunately, the limited size of the data base currently available for these parameters precludes the definition of pedo-transfer functions for their spatial extension [*Hénault et al.*, 2005]. We thus simply applied the values obtained in the test site to the whole sub-region, considering these sites representative of this area. The influence of this hypothesis on the final results was tested in the uncertainty analysis.

#### 2.2.3. Model running

CERES-EGC was run in each of the elementary simulation units for a reference period running from mid-September, 1998, to mid-September, 1999. Initial moisture content was set at 90% of the field-capacity content throughout the soil profile, based on simulations of the preceding cropping season. Initial nitrate and ammonium concentrations in the soil were set at 5 and 1 mg N $kg^{-1}$ soil, respectively, throughout the profile. It corresponds to a total residual mineral N content of 80 kg N $ha^{-1}$ in the top 1 m of soil, which is the average of N stocks measured in the region at that time of year (B. Nicoullaud, unpublished data, 2003). Annual N deposition was neglected, being less than 4 kg N $ha^{-1}$ in the area [*Ulrich and Willot*, 1993]. Since the focus was on wheat-cropped soils, the area of the simulation units were corrected for the fraction of land cropped to wheat in these units. Aggregation of elementary fluxes within each sub-region yielded the total $N_2O$ efflux estimated from winter wheat crops over this sub-region.

Wheat management data was set according to the recommendations made by local advisory services [*Germon et al.*, 2003]. The mean doses of fertilizer N were 195 kg N $ha^{-1}$ in Beauce Dunoise and 215 kg N $ha^{-1}$ in Faux-Perche and Beauce Chartraine, split into three applications in spring. Only mineral fertilizers were considered (in the form of ammonium nitrate and urea), since organic forms are applied on only 2% of the cropland area in the region studied here, and make up less than 2 % of the total amounts of fertilizer N applied.

#### 2.2.4. Sensitivity and uncertainty analysis

Extrapolating model simulations from plot to regional scale involves two main sources of uncertainty [*Butterbach-Bahl et al.*, 2004], which may be considered independent: i/ uncertainties in model inputs, including parameters, driving variables (climate and crop management), and initial conditions, and ii/ model prediction error.

To address the first source, we ran a simple, local sensitivity test in which the inputs were varied one-at-a-time over their plausible range while keeping the others at their nominal value. We subsequently estimated a probability density functions (pdfs) for the most sensitive inputs, and evaluated their combined effect on the variance of model predictions using winding stairs sampling [*Jansen et al.*, 1994]. The method is a modified Latin Hypercube sampling which makes it possible to estimate the contribution of individual inputs ($X_i$) to the total variance in model output ($Y$) using variance ratios. For instance, the 'top marginal variance' (TMV) is defined as: $TMV = Var(E(Y \mid X_i = x_i))/Var(Y)$, where Var and E denote the variance and expectancy, respectively. The TMV indicates the mean reduction of

$Var(Y)$ made possible by setting input $X_i$ at its nominal value $x_i$, *i.e.* imposing $Var(X_i) = 0$.
All analyses were done at the sub-regional scale, the output variable of interest ($Y$) being the simulated $N_2O$ efflux.

The second source of uncertainty (model error) was estimated as mean squared error achieved by CERES-EGC in the prediction of annual $N_2O$ fluxes in the three test sites, using the regional parameterization (see below section). Ultimately, the total uncertainty on the predicted sub-regional efflux was calculated as the sum of the variances related to input uncertainties and to model error.

#### 2.3. Local test sites

One test site was set up in each sub-region to check the simulations of $N_2O$ emissions obtained with the regional parameterization procedure detailed in section 2.2.2. The sites were selected as representative of the sub-region, and involved a Haplic Luvisol in Beauce Chartraine (site name: La Saussaye; 4824'N, 134'E), a Haplic Calcisol in Beauce Dunoise (at Villamblain; 4798'N, 134'E), and a Gleyic Luvisol in Faux-Perche (at Arrou; 4808'N, 106'E) - FAO classification [*ISSS/ISRIC/FAO*, 1998].
$N_2O$ emissions were monitored by the static chamber method using circular chambers (0.5 m in diameter and 0.15 m in height), with 8 replicates [*Hénault et al.*, 2005]. Other outputs were also monitored to test the simulation of intermediate variables. Topsoil water content was continuously recorded using TDR probes, soil nitrogen content was measured every two weeks in the topsoil and every month in the subsoil, and plants were regularly sampled and analyzed for aerial dry matter, leaf area and nitrogen content. Lastly, a weather station was set up to record the data required by CERES-EGC (rainfall, air temperature and solar radiation), along with soil temperature.
Detailed information was also collected to supply the soil parameters of CERES-EGC. Hydrodynamic parameters (water retention and hydraulic conductivity curves) were measured on intact cores taken to the laboratory. Site-specific parameters required by the $N_2O$ module were also measured in the laboratory, following the procedures given in section 2.2.3.
These data sets were used to test the implementation of the $N_2O$ modules within CERES-EGC in a previous paper *Gabrielle et al.* [2006]. Here, they served to test the 'regional' parameterization method described in section 2.2.2, against the baseline, more detailed 'local' parameterization resulting from the above measurements. In the test sites, model fit to observed data was evaluated by calculating the mean deviation (MD) and the root mean squared error (RMSE), defined as: $MD = E(O_i - S_i)$ and $RMSE = (E[(O_i - S_i)^2])^{1/2}$, where $S_i$ and $O_i$ are the time series of the simulated and observed data. Model error in the prediction of yearly cumulative (as opposed to daily instantaneous) $N_2O$ fluxes was assumed proportional to the simulated flux, and estimated as [*Smith et al.*, 1996]:
$RMSE_{yr} = 100/E(O_{i,s}) \times [E(MD_s^2)]^{1/2}$,
where $MD_s$ are the mean deviations in the test sites, and $O_{i,s}$ the daily observations in these sites.

## 3. Results

#### 3.1. Simulations in the three test sites

Figure 1 compares the simulations obtained with the regional parameterization procedure in the three test sites with those resulting from the detailed soil characterization, which was used to implement the $N_2O$ module of CERES-EGC [*Gabrielle et al.*, 2006]. In one of the sites (Villamblain), the potential denitrification rate had to be reduced by a factor of 5 in order to obtain an acceptable fit to observed emission rates. Thus, this parameter was set at 3.4 kg $N_2O$-N ha$^{-1}$ yr$^{-1}$ in the surrounding sub-region, namely Beauce Dunoise.
The local and regional parameterization scenarios yielded similar temporal dynamics in all sites. However, closer examination revealed some differences in the magnitude of the emission peaks simulated. Compared to the local parameterization, the regional one resulted in lower fluxes after spring fertilization at Arrou and Villamblain, and higher fluxes in La Saussaye. As a result, the $N_2O$ emissions predicted by the regional parameterization scenarios differed by -40% to

**Table 2.** Cumulative annual $N_2O$ emissions (kg $N_2O$-N ha$^{-1}$ yr$^{-1}$) simulated with the local and regional regional parameterization procedures, along with statistical indicators of model fit to observed data. The hypothesis that the mean deviation is zero was tested using a two-tailed t-Test, and the root mean squared error is compared to mean experimental error using an F variance test [*Smith et al.*, 1996].

| | La Saussaye | | Villamblain | | Arrou | |
|---|---|---|---|---|---|---|
| Parameterization scenario | Regional | Local | Regional | Local | Regional | Local |
| Annual $N_2O$ flux (kg $N_2O$-N ha$^{-1}$ yr$^{-1}$) | 5.08 | 3.29 | 5.45 | 2.39 | 3.85 | 6.64 |
| Mean deviation (g $N_2O$-N ha$^{-1}$ d$^{-1}$) | 0.61[a] | -0.95[a] | 0.56[a] | -1.24[a] | 8.84[a] | 5.57[a] |
| Root mean squared error (g $N_2O$-N ha$^{-1}$ d$^{-1}$) | 4.99[b] | 8.04 | 6.43[b] | 9.00[b] | 34.1 | 38.4 |

[a] not significantly different from zero (p=0.05)
[b] not significantly greater than experimental error (p=0.05)

+130% relative to the local parameterization, when accumulated over the simulation period (Table 2).

These discrepancies were mostly due to differences regarding soil water retention properties and bulk density, to which the model proved very sensitive. At La Saussaye, for instance, topsoil bulk density differed by only 0.08 g $cm^{-3}$ between the two parameterizations, but this was enough to create a 30% deviation in terms of simulated $N_2O$ efflux. Despite these discrepancies, the mean deviations (MD) and root mean squared errors (RMSE) achieved by the two parameterization scenarios were generally close, the only notable difference being that the RMSE was significantly higher with the regional parameterization than with the local one at Arrou. The mean deviation was also relatively high for this site (amounting to 8 g $N_2O$-N $ha^{-1}$ $d^{-1}$), compared to the other two sites in which it was negligible. As a result, the estimated relative error for the annual simulated flux ($RMSE_{yr}$) amounted to 64%.

### 3.2. Regional simulations

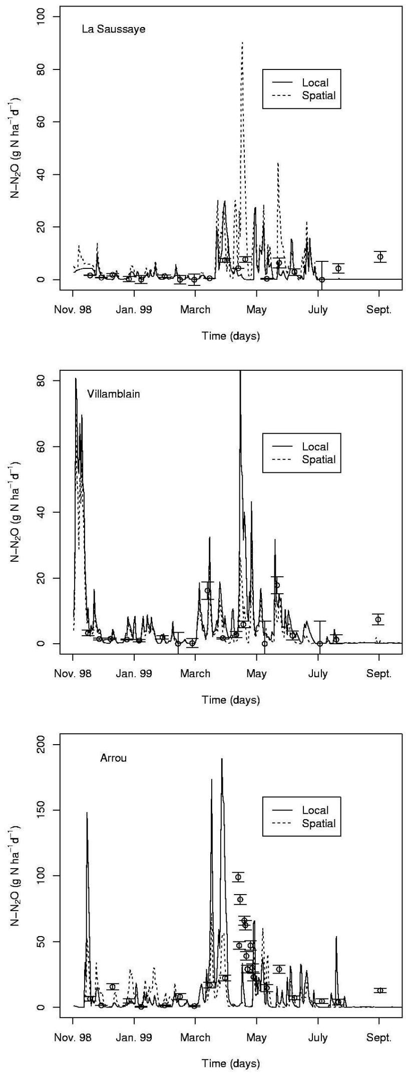


**Figure 1.** Simulated (lines) and observed (symbols) emissions of $N_2O$ in the three test sites. In the local parameterization scenario, detailed, site-specific information on soil properties was used, whereas the regional scenario involved only information derived from the soil map.

**Table 3.** Emissions of $N_2O$ simulated within each sub-region (total and average per hectare), with a standard or zero dose of fertilizer N. Regional estimates obtained with the IPCC methodology are also reported (corresponding to the emissions due to fertilizer application).

| Sub-region | Total area simulated | Fertilizer N dose | Mean annual $N_2O$ flux | Regional flux | Regional Emission Factor |
|---|---|---|---|---|---|
| | ha | kg N ha$^{-1}$ | kg $N_2O$-N ha$^{-1}$ | kg $N_2O$-N | kg $N_2O$-N kg$^{-1}$ N |
| Beauce | 31,927 | 215 | 1.37 | 42,887 | 0.0016 |
| Chartraine | | 0 | 1.02 | 31,868 | |
| **IPCC** | 31,927 | 215 | 3.69 | 117,810 | 0.0125 |
| Beauce | 23,474 | 195 | 0.65 | 15,384 | 0.0007 |
| Dunoise | | 0 | 0.52 | 12,165 | |
| **IPCC** | 23,474 | 195 | 3.44 | 80,750 | 0.0125 |
| Faux- | 16,578 | 215 | 2.23 | 37,010 | 0.0033 |
| -Perche | | 0 | 1.51 | 25,062 | |
| **IPCC** | 16,578 | 215 | 3.69 | 61,172 | 0.0125 |

Table 3 summarizes the simulation outputs for the three sub-regions, while Figure 3 provides a geographical mapping of the emissions. In terms of spatial distribution, there were no marked differences between the sub-regions, which all presented a wide range of emission rates. Beauce Chartraine exhibited a longitudinal gradient with lower $N_2O$ fluxes to the East and higher fluxes to the West, whereas in Faux-Perche the emission levels were vertically stratified from North to South. Conversely, Beauce Dunoise was rather homogeneous and centered in the mid-range values of $N_2O$ fluxes. When expressed per unit area, the mean $N_2O$ fluxes varied markedly across the regions, from 0.63 kg $N_2O$-N ha$^{-1}$ yr$^{-1}$ in Beauce Dunoise to 2.23 kg $N_2O$-N ha$^{-1}$ yr$^{-1}$ in Faux-Perche. This range was much lower than the 3.85 - 5.45 kg $N_2O$-N ha$^{-1}$ yr$^{-1}$ simulated in the test sites with the regional parameterization.

Within the sub-regions, the western half of Beauce Chartraine appeared particularly sensitive in the regional balance of $N_2O$ emissions. Other zones prone

**Table 4.** Sensitivity of model-predicted $N_2O$ efflux in the Beauce Dunoise sub-region to selected inputs. Soil parameters pertain to the top layer (0-30 cm). Site-specific inputs were assigned a fixed coefficient of variation (CV, in %), and varied within their 95% confidence interval, while inputs considered constant at the sub-regional level were given an overall variation range. Model response is expressed as changes in model output relative to the baseline input setting.

| Symbol | Description (Unit) | Variation range / CV | Source | Model response (change relative to baseline) |
|---|---|---|---|---|
| SOIL PARAMETERS | | | | |
| OC | organic carbon content (g g$^{-1}$ soil) | 15% | 1 | -1.7% to +2.2% |
| pH | pH in water | 8% | 1 | -0.3% to +2.1% |
| BD | Topsoil bulk density (g cm$^{-3}$) | 5% | 2 | -80% to +321% |
| $K_{sat}$ | Saturated hydraulic conductivity (m d$^{-1}$) | 50% | 3 | -1.3% to +1.9% |
| $\theta_{fc}$ | Soil water content at field-capacity (g g$^{-1}$ soil) | 10% | 4 | -72.5% to +250% |
| PDR | Potential denitrification rate (kg N ha$^{-1}$ d$^{-1}$) | 3.4 – 15.7 | 5 | -71% to 0% |
| $r_D$ | Fraction of denitrification evolved as $N_2O$ (%) | 20 – 64 | 5 | 0% to +290% |
| DRIVING VARIABLES | | | | |
| R | Annual rainfall (mm yr$^{-1}$) | 10% | 6 | -22.3% to +27.2% |
| INITIAL CONDITIONS | | | | |
| $I_N$ | Mineral N in soil profile (top 1 m; kg N ha$^{-1}$) | 40 – 125 | 6 | -24.1% to +31.4% |
| $I_w$ | Moisture content in soil profile (top 1 m; mm) | 50 – 150 | 6 | -6.7% to +1.8% |

1: Variability within soil type units; 2: Measurement error; 3: Range covered by each $K_{sat}$ class; 4: Prediction error of pedo-transfer function [*Bastet et al.*, 1998]; 5: Range across the 3 test sites; 6: Intra-regional variability [Nicoullaud, B. (unpublished data, 2003)].

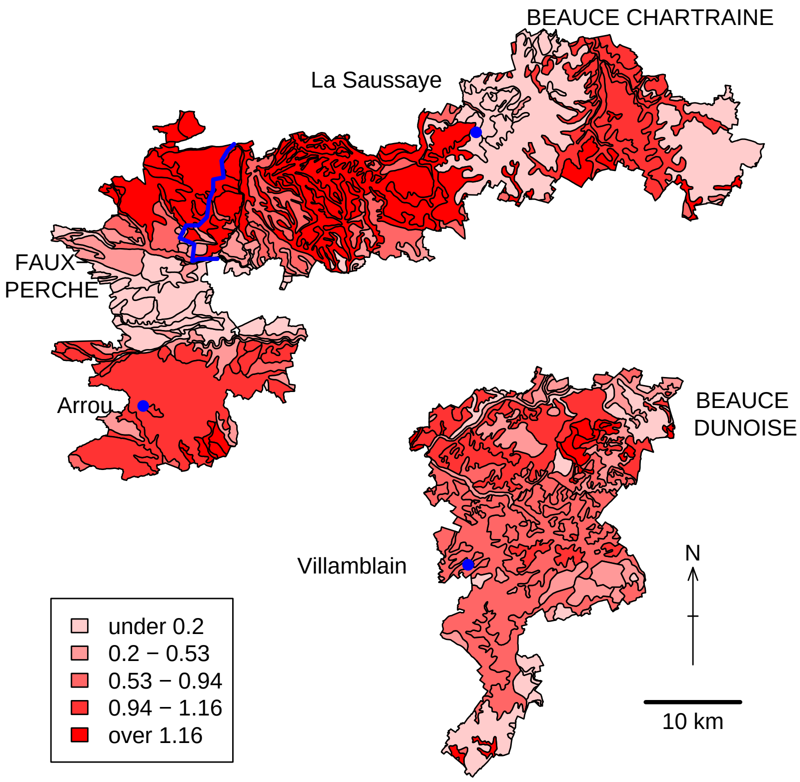


**Figure 3.** Simulation of $N_2O$ emissions from wheat-cropped land in three agricultural sub-regions of the Beauce region. The fluxes are expressed in kg $N_2O$-N $ha^{-1}$ $yr^{-1}$.

to $N_2O$ emissions zones could also be delineated, such as the northernmost and southernmost tips of Faux-Perche. Spatial structures in the other parts of the map were mostly determined by the spatial resolution of the soil map units (SMU), some of which were rather large with sizes ranging up to 19,000 ha. In addition, SMUs were made up of two to five different soil type units (STUs), with possibly contrasting potentials for $N_2O$ emission. On the other hand, emissions were much less variable within a given STU when it occurred across several map units and thereby climatic conditions. Figure 2 shows the distribution of fluxes across the various STUs to be strongly skewed, with an extended tail in the higher range of emissions (> 5 kg N $ha^{-1}$ $yr^{-1}$). However, the weight of this upper-tail was very limited, comprising only 11 STUs out of a total of 230, and making up 0.7% of the total area simulated.

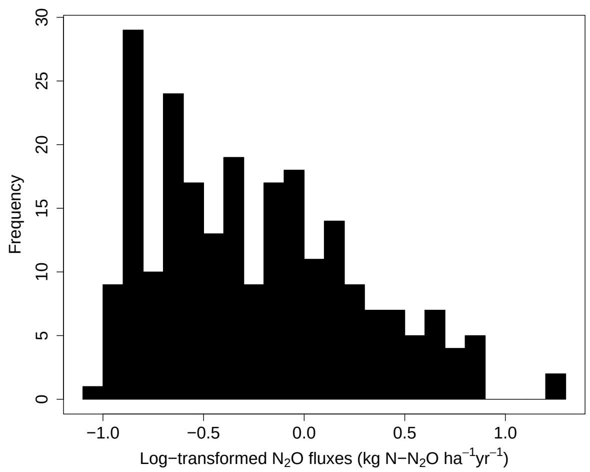


**Figure 2.** Histogram of log-transformed simulated fluxes across the various soil type units in the three sub-regions.

### 3.3. Sensitivity analysis

Table 4 lists the parameters included in the sensitivity analysis, along with their standard deviations or variation ranges. Model response to changes in these inputs is given only in the case of Beauce Chartraine, but similar patterns were noted in the other two sub-regions (not shown).
Overall, the two microbiological parameters governing $N_2O$ emissions (PDR and $r_D$) were among the the four most sensitive inputs. When varied across their inter-regional range, they introduced a one- to three-fold variation in the predicted $N_2O$ efflux. This could be expected since there was a factor of 5 between the minimum and maximum values of PDR, and a factor of 3 for $r_D$. Also, given the nature of the denitrification equations, the model responded linearly to changes in these parameters. Soil bulk density (BD) was the next most influential parameter, as already noted in the local test sites. A 10% relative variation of BD entailed more than much higher relative changes in model output, ranging from -80% to 320%. This is due to the markedly convex power function used in the model to relate the water-filled pore space (WFPS) to denitrification [*Hénault and Germon*, 2000]. Increasing bulk density decreases soil porosity and thereby the threshold moisture content above which denitrification is activated, which corresponds to 62% WFPS. It therefore increases the probability of moisture conditions conducive to denitrification and $N_2O$ emissions. For the same reason, the field-capacity water content ($\theta_{fc}$) also proved sensitive, but to a lesser extent. Surprisingly, the saturated hydraulic conductivity had very little effect, despite being varied over a wide range (± 50%). It is probably because the dynamics of topsoil water were mostly governed by the field-capacity content, at least for water contents close to saturation, as previously reported with the CERES water balance routine [*Gabrielle et al.*, 1995].

The model was insensitive to topsoil organic C content and pH, because unlike other models [*Parton et al.*, 2001; *Li et al.*, 2001], it does not explicitly include these factors as controls in the production and reduction of $N_2O$. Their influence is only indirect, via the processes of ammonia volatilization (for soil pH) and the mineralization/immobilization of soil N (for soil organic C). Initial soil water and N content appeared little to moderately sensitive, respectively. There was a -24% to +31% change in the sub-regional $N_2O$ flux over the range of initial N contents. The influence of initial water content was more marginal, probably because the simulations started two months ahead of the wetter winter season. On the other hand, changes in annual rainfall affected soil water content throughout the simulation period, and rainfall appeared as sensitive as initial N content as a result.

### 3.4. Uncertainty analysis

**Table 5.** Statistics of the sub-regional $N_2O$ fluxes generated by winding stairs sampling of 5 parameters. The coefficient of variation (CV) was estimated on the truncated distribution ($0.025 \leq p \leq 0.975$).

| Sub-region | Median | 95% confidence interval | CV |
|---|---|---|---|
| | Mg $N_2O$-N $yr^{-1}$ | | % |
| Beauce Chartraine | 118.1 | 21.2 – 497.2 | 109% |
| Beauce Dunoise | 125.0 | 15.0 – 561.2 | 123% |
| Faux-Perche | 49.4 | 9.8 – 213.0 | 113% |

Based on the above results, 5 parameters were selected for the uncertainty analysis: PDR, $r_D$, BD, $\theta_{fc}$,

and initial soil N content ($I_N$). We used truncated Gaussian pdfs ($0.025 \leq p \leq 0.975$) for the last 3 inputs, considered site-specific, and uniform pdfs for the first two, taken as constant within each sub-region. A correlation coefficient of -0.52 between the field-capacity water content and bulk density was introduced, according to the finding of *Bastet et al.* [1998].
The distributions of $N_2O$ fluxes generated with the winding stairs sampling (WSS) of these inputs were log-normal, with an extended tail in the higher range of values and a large variance (Figure **??**). Table 5 shows the median and 95% confidence intervals calculated in the three sub-regions. In all of them, the median fluxes were larger than the baseline values of Table 3. This was expected in Beauce-Chartraine and Beauce Dunoise, given that in the baseline parameterization they were assigned the lowest values for $r_D$ and/or PDR. Since the pdfs of these two parameters were centered on their mid-range estimates, the fluxes generated by sampling in these pdfs could only be higher than with the baseline setting. However, Faux-Perche presented an opposite situation since its baseline value of $r_D$ was the higher bound of its sampling range (64%). The fact that the WSS-generated median $N_2O$ flux was still higher than its baseline value evidences the influence of the site-specific parameters ($\theta_{cf}$, $I_N$ and BD), and also strong non-linearity with the model.

There was ample variation around the median: the lower and upper 95% confidence limits corresponded to 18-20% and 420-450% of the median, respectively, and the coefficients of variations ranged from 109% to 123%. Compounding this variability with the estimated model prediction error (assuming both variates to be log-normal), the lower and upper limits of the 95% confidence were estimated as 33% and 300% of the mean predicted flux, respectively. Lastly, the calculation of top marginal variances (TMV) made it possible to estimate the contribution of individual inputs to the total variance. Soil physical parameters (BD and $\theta_f c$) explained 62% to 75% of the total variance, while the microbiological parameters (PDR and $r_D$) had a contribution ranging from 12% to 30%, and the initial nitrate content only had a marginal role. This ranking differs from that output by the one-at-a-time sensitivity test (Table 4), evidencing interactions between inputs that amplified model response to physical parameters while drastically reducing the influence of initial conditions.

### 3.5. Sensitivity to fertilizer N

At the sub-regional level, the model-based estimates of direct $N_2O$ emissions from wheat-cropped fields were 39% to 81% lower than the IPCC ones. The deviation was strongest in Beauce Dunoise and smallest in Faux-Perche, reflecting the ranking of the sub-regions respective to $N_2O$ emissions on a per hectare basis. The background emissions simulated by CERES-EGC were also lower than the IPCC default value of 1 kg $N_2O$-N $ha^{-1}$, but to a lesser extent than the total emissions, and ranged from 0.52 to 1.02 kg $N_2O$-N $ha^{-1}$. As a result, model-based $EF_d$ estimates were extremely low compared to the IPCC default ($0.0125 \pm 0.01$ kg $N_2O$-N $kg^{-1}$ N), ranging from 0.0007 to 0.0033 kg $N_2O$-N $kg^{-1}$ N. This low sensitivity of model results to fertilizer N essentially arose from the fact that a major fraction of the emissions happened outside the spring season during which fertilizer was applied. Some emissions occurred prior to wheat planting in the fall of 1998, as may be seen on Figure 1, or in the late summer and fall of 1999. Because wheat crops actively took up soil N during their growing season, fertilization actually had little influence on the soil inorganic content upon harvest in summer, and on the subsequent emissions of $N_2O$.

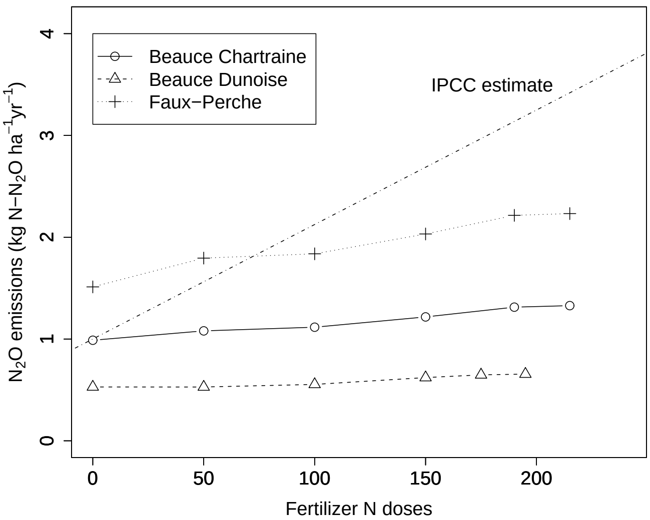


**Figure 4.** Simulated relationships between fertilizer N dose and year-round $N_2O$ emissions at the sub-regional level. The straight line corresponds to the *IPCC* [1997] relationship.

Secondly, $N_2O$ emissions were generally proportional to the amount of fertilizer N applied to crops, whatever the range of fertilizer doses (Figure 4). As a result, the average $EF_d$s estimated by fitting a straight line to the response curve provided estimates nearly identical to those obtained by using emissions data only for the nominal and zero doses of fertilizer N, as is usually done in the IPCC method.

## 4. Discussion

### 4.1. Uncertainty and validity of regional estimates

Extrapolating model simulations from plot to regional scale involves some degree of uncertainty in spatialized inputs as well as model robustness to spatial extension. The uncertainties of a range of inputs could be quantified prior to extrapolation, and their effects approached via sensitivity and uncertainty analyses (UA). The setting of microbiological parameters (PDR and $r_D$) proved most crucial in the regional extension, being both sensitive and highly uncertain. Unfortunately, they could not be spatialized based on the available soil information because they do not yet appear to be related to particular physico-chemical properties, such as soil texture or organic matter content [*Hénault et al.*, 2005]. For lack of an alternative method, we assumed in the baseline parameterization that the values of PDR and $r_D$ measured in each test site could apply to the entire surrounding sub-region. This hypothesis of a strong spatial structure in the distribution of soil microbiological properties was based on the pedoclimatic zoning of the sub-regions. However, it may appear somewhat arbitrary, and was actually tested against a null hypothesis by which microbiological properties were randomly distributed across the sub-regions within their overall variation ranges. The difference between the two parameterizations turned out to be extremey large: the median $N_2O$ effluxes calculated in the UA were 1.2- to 8-fold higher than with the baseline parameterization. Better knowledge of the spatial determinants of those parameters is therefore paramount to reducing the uncertainty of such model-based estimates.

Topsoil bulk density was also very sensitive, but its contribution to the total variance was somewhat reduced because of its correlation with the field-capacity water content. Although the wide body of literature currently available on the estimation of these parameters makes it possible to narrow down their range of uncertainty, it is notable that they contributed nearly as much variance to the $N_2O$ fluxes as the microbiological parameters. This contribution of water content was also noted by *Mummey et al.* [1998], who reported a 1.3- to 2-fold increase in $N_2O$ emissions from arable crops when increasing soil water content by 40%. In addition, because the variation ranges chosen for these parameters fall within their spatial variations at the field-scale [*Yanai et al.*, 2003], it is likely that this source of error will remain as a background noise in the predictions of $N_2O$.

Lastly, the fact that the model was sensitive to the initial soil N content points at a possible strategy for reducing $N_2O$ emissions. A target initial content of 40 kg N $ha^{-1}$ (down to 1 m) would indeed make it possible to reduce the emissions by 25%, which is more than what could be achieved by a drastic reduction of fertiliser N application to the following crop. Best management practices may in principle make it possible to reach such a target [*Loyce et al.*, 2002].

The second major source of uncertainty (model robustness to spatial extension) could be judged from the mean deviations achieved by CERES-EGC in the test sites with the regional parameterization. These errors ranged from 0.5 to 8.4 g $N_2O$-N $ha^{-1}$ $d^{-1}$, which represents 7% to 50% of the mean observed fluxes (Table 2). This range may be taken as the error margin associated with the simulation of the annual $N_2O$ efflux by the model. When compounded over the three sites, the average relative prediction error was estimated at 64%, because one of the test sites (Arrou) had much higher fluxes than the other two. From a more qualitative viewpoint, the extent to which CERES-EGC could be extrapolated to new field situations may be judged based on its $N_2O$ sub-model, NOE. The latter was successfully tested in 3 field sites in France, other than the 3 test sites involved here, along with 3 field sites in Central America [*Hénault et al.*, 2005]. In these sites the mean daily emission rates varied between 2 to 50 g $N_2O$-N $ha^{-1}$ $d^{-1}$, thus encompassing the 8-9 g $N_2O$-N $ha^{-1}$ $d^{-1}$ range that could be expected in the sub-regions based on the IPCC approach (Table 3).

Regional estimates based on bottom-up aggregation of plot-scale fluxes generally involve model testing in a few test sites, and direct extrapolation to the area of interest [*Li et al.*, 2001; *Mummey et al.*, 1998]. Because testing usually involves site-specific calibration of some model parameters [*Frolking et al.*, 1998; *Gabrielle et al.*, 2002], we included here an intermediate phase in which the default parameterization procedure applied at the regional scale was compared with a more detailed, site-specific parameterization. Of course, this comparison also involves a scaling issue, since the soil typological units (STUs) used in the regional parameterization were much larger than the area covered by the measurements in the test sites. As a result, the discrepancies between the model outputs using whether the site-specific or the regional parameterization should not be taken as a failure of the model, but rather as an indication of the degree of uncertainty associated when downscaling from the soil mapping unit (SMU) to the plot-scale. It is also noticeable that they produced an acceptable fit to the measurements (Table 2).

Overall, combining the unknowns mentioned above resulted in 95% confidence limits representing 33% and 300% of the mean simulated estimates, respectively. This is much larger than the ±80% confidence interval of the IPCC methodology, and the ± 50% interval reported by *Li et al.* [2001] in their inventory based on the DNDC model, but it encompasses more sources of uncertainty - including, most notably, model prediction error.

### 4.2. Empirical and model-based emission factors

There is a growing body of literature on the determination of direct emission factors (EF*d*s) from field measurements at the plot-scale. These factors have been shown to be extremely variable from one field to the other, ranging from 0.0003 to 0.068 kg $N_2O$-N $kg^{-1}$ N [*Flessa et al.*, 2002; *Velthof et al.*, 2003; *Kaiser et al.*, 1998; *Zheng et al.*, 2004]. There are many sources of uncertainty behind these empirical estimates: quantification of background emissions, spatial and temporal coverage, and time-frame on which the measurements are carried out, which all warrant corrections [*Zheng et al.*, 2004]. According to the latter, the absence of background emissions data is expected to lead to an over-estimation of $EF_d$s, by 15% to 110% under Chinese conditions. Conversely, a shortage of temporal coverage (insufficient frequency of measurements) would lead to an under-estimation by 19% to 30%.

Process-based models should not require any such corrections since they simulate $N_2O$ emissions continuously over time, and can predict fertilized as well as unfertilized crops. Thus, they may be expected to supply $EF_d$ values up to 80% lower than the empirical estimates listed above, among which the IPCC methodology. Such was the case with the $EF_d$s simulated with CERES-EGC, which fell in the lower range of the IPCC values. Similarly, another modeling study reported an average $EF_d$ of 0.008 kg $N_2O$-N $kg^{-1}$ N with a 0.0025-0.04 kg $N_2O$-N $kg^{-1}$ N range for cropland in China [*Li et al.*, 2001]. Calculation of $EF_d$s without the control term (ie assuming zero emissions for unfertilized crops), as was done in a number of studies for lack of background emissions data [*Zheng et al.*, 2004], resulted in $EF_d$s ranging between 0.0033 and 0.0104 kg $N_2O$-N $kg^{-1}$ N. This falls within the lower half of the IPCC range (0.0025 to 0.0225 kg $N_2O$-N $kg^{-1}$ N).

Fertilizer type is also mentioned to affect the values of $EF_d$, although there is a lack of sufficient data to derive generic, fertilizer-specific figures [*Bouwman*, 1996; *Mosier et al.*, 1996]. *Bouwman* [1996] reported $EF_d$ values of 0.003 ± 0.003 kg $N_2O$-N $kg^{-1}$ N for ammonium nitrate and urea, the two types of fertilizers used in the sub-regions simulated here.

Lastly, $EF_d$s should capture some range of inter-annual variability. It is in principle possible with a model like CERES-EGC, but we considered it beyond scope here since we focused on spatial extension from plot-scale to regional scale. However, our results are to a large extent conditioned by the growing season in which the experiments and simulations were run. Investigating the effect of inter-annual climate variability is therefore a major prospect for future work on $N_2O$ simulations.

### 4.3. Factors controlling $N_2O$ emissions at the regional scale

Two major differences occured between the model-based and IPCC estimates of $N_2O$ emissions at the sub-regional scale: the magnitude of the emissions, and the response to fertiliser N. Both appeared much weaker with the model, and are discussed below. The lack of response to fertilization essentially occured because the simulated $N_2O$ emissions were not concentrated in the spring season when fertilizer was applied. However, it may also be a result of the upscaling from field- to regional-scale. The literature on spatial extension of $N_2O$ fluxes, whether using process-based models or more empirical methods, shows the 'fertilizer dose' factor to lose some influence in favor of environmental characteristics, as the spatial area increases. At the European scale, *Freibauer* [2003] modeled $N_2O$ emissions based on pedological and agronomic factors, and found a coefficient of only 0.4% in the correlation between these emissions and fertilizer doses. In a review of emission data covering a wide range of crop management and geographical locations, *Kaiser et al.* [1998] report a similar coefficient with a value of 0.6%. These figures could be interpreted as an average $EF_d$ of 0.004 to 0.006 kg $N_2O$-N $kg^{-1}$ N for Europe. The apparent discrepancy between the ranges of $EF_d$s obtained at the plot and regional scales may be due to an uneven sampling of field sites biased towards the more $N_2O$-productive sites, when establishing empirical $EF_d$s, and these sites might turn out to represent only a small proportion of total arable land. Such was the case in our study since the test sites were actually above average in terms of $N_2O$ emissions. The frequent lack of background data in these experiments is also a source of bias since a significant part of the emissions attributed to fertilizer use might actually be related to the soil potential per se, as happened in our simulations. For urea and ammonium-nitrate type fertilizers, *Bouwman* [1996] reported relative differences as high as 100% between $EF_d$ estimates including or not an unfertilized control.

Regarding the magnitude of the simulated fluxes, the study by *Li et al.* [2001] at the country level revealed a clustered spatial pattern for $N_2O$ emissions, with contrasting efflux rates between groups of counties (equivalent to our sub-regions). It is thus probable that some sub-regions would contribute significantly less $N_2O$ than others, which seems to be the case with those we had selected here. On the other hand, the IPCC $EF_d$ are representative at a global or continental scale, as they were obtained from observations worldwide, rather than at the sub-regional level. Overall, in our sub-regions, $N_2O$ emission levels primarily depend on a local potential set by climatic conditions combined with soil microbiological and physical properties, with the influence of crop management appearing somewhat minor in the expression of this potential. As a consequence, reducing fertilizer N would seemingly have little effect on abating $N_2O$ fluxes. However, the fertilizer dose also influences the residual mineral N content upon sowing of the proceeding crop, which significantly affected the sub-regional $N_2O$ efflux.

As a conclusion, under such mild temperate climatic conditions as investigated here, mitigation measures should target a reduction in the amount of soil mineral N in autumn, and a decrease of the soil $N_2O$ production potential itself. While there is a range of best management packages available to address the first point, there is a need for future research on the microbial and physical determinants of soil emission potentials, and how they may be affected by crop management.

**Acknowledgments.** Financial support from the French Ministry for the Environment (through its GESSOL grant program) is acknowledged. The authors would like to thank two anonymous referees for stimulating comments on the manuscript.

## References


Arrouays, D., W. Deslais, J. Daroussin, J. Balesdent, J. Gaillard, J. L. Dupouey, C. Nys, V. Badeau, and S. Belkacem (1999), Stocks de carbone dans les sols de France. Quelles estimations?, *CR. Acad. Agric. F.*, *85*, 278–292.

Bastet, G., A. Bruand, P. Quétin, and I. Cousin (1998), Estimation des propriétés de rétention en eau des sols à l'aide de fonctions de pédo-transfert (FPT), *Et. Ges. Sols*, *5*, 7–28.

Bouwman, A. (1996), Direct emissions of nitrous oxide from agricultural soils, *Nutr. Cycl. Agroecos.*, *46*, 53–70.

Butterbach-Bahl, K., M. Kesik, P. Miehle, H. Papen, and C. Li (2004), Quantifying the regional source strength of N-trace gases across agricultural and forest ecosystems with process based models, *Plant Soil*, *260*, 311–329.

Duxbury, J. M., and D. R. Bouldin (1982), Emission of nitrous oxide from soils, *Nature*, *298*, 462–464.

Flessa, H., R. Ruser, P. Dorsch, T. Kamp, M. Jimenez, and J. C. Munch (2002), Integrated evaluation of greenhouse gas emissions ($CO_2$, $CH_4$, $N_2O$) from two farming systems in southern Germany, *Agric. Ecosys. Environ.*, *91*, 175–189.

Freibauer, A. (2003), Regionalised inventory of biogenic greenhouse gas emissions from European agriculture, *Eur. J. Agron.*, *19*, 135–160.

Frolking, S. E., A. R. Mosier, D. S. Ojima, C. Li, W. J. Parton, C. S. Potter, E. Priesack, R. Stenger, C. Haberbosch, P. Dörsch, H. Flessa, and K. A. Smith (1998), Comparison of N2O emissions from soils at three temperate agricultural sites: simulations of year-round measurements by four models, *Nutr. Cycl. Agroecos.*, *52*, 77–105.

Gabrielle, B., S. Menasseri, and S. Houot (1995). Analysis and field-evaluation of the CERES models' water balance component, Soil Sci. *S*oc. Am. J., 59, 1402–1411.

Gabrielle, B., R. Roche, P. Angas, C. Cantero-Martinez, L. Cosentino, M. Mantineo, M. L. an C. Hénault, P. Laville, B. Nicoullaud, and G. Gosse (2002), A priori parameterisation of the ceres soil-crop models and tests against several european data sets, *Agronomie 22: 119-132*.

Gabrielle, B., P. Laville, C. Hénault, B. Nicoullaud, and J. C. Germon (2006), Simulation of nitrous oxide emissions from wheat-cropped soils using CERES, *Nutr. Cycl. Agroecos.*, *74*, 133 – 146, doi:10.1007/s10705-005-5771-5.

Garrido, F., C. Henault, H. Gaillard, S. Perez, and J. C. Germon (2002), $N_2O$ and NO emissions by agricultural soils with low hydraulic potentials, *Soil Biol. Biochem.*, *34*, 559–575.

Germon, J. C., C. Hénault, P. Cellier, D. Chèneby, O. Duval, B. Gabrielle, P. Laville, B. Nicoullaud, and L. Philippot (2003), Les émissions de protoxyde d'azote ($N_2O$) d'origine agricole. Evaluation au niveau du territoire français., *Et. Ges. Sols*, *10*, 315–328.

Grant, R. F., and E. Pattey (2003), Modelling variability in $N_2O$ emissions from fertilized agricultural fields, *Soil Biol. Biochem.*, *35*, 225–243.

Hénault, C., and J. C. Germon (2000), NEMIS, a predictive model of denitrification on the field scale, *Eur. J. Soil Sci.*, *51*, 257–270.

Hénault, C., D. Chèneby, K. Heurlier, F. Garrido, S. Perez, and J. Germon (2001), Laboratory kinetics of soil denitrification are useful to discriminate soils with potentially high levels of $N_2O$ emission on the field scale, *Agronomie*, *21*, 713–723.

Hénault, C., F. Bizouard, P. Laville, B. Gabrielle, B. Nicoullaud, J. C. Germon, and P. Cellier (2005), Predicting *in situ* soil N2O emissions using NOE algorithm and soil data base, *Global Change Biol.*, *11*, 115–127.

IPCC (1997), *Guidelines for national greenhouse gas inventories: greenhouse gas inventory reference manual, revised 1996*, IPCC/OECD/IGES, Bracknell, UK.

Isambert, M. (1984), Carte pédologique 1/100 000 de Châteaudun. Notice explicative, *Tech. rep.*, INRA Edition, Paris.

ISSS/ISRIC/FAO (1998), *World Reference Base for soil resources*, *World Soil Resources Rep.*, vol. 84, FAO, Rome.

Jansen, M. J. W., W. A. H. Rossing, and R. A. Daamen (1994), Monte Carlo estimation of uncertainty contributions from several independent multivariate sources, in *Predictability and nonlinear modelling in natural sciences and economics*, edited by J. Grasman and G. van Straten, pp. 335–343, Kluwer Academic Publ., Dordrecht, N.L.

Jones, C. A., and J. R. Kiniry (1986), *Ceres-N Maize: a simulation model of maize growth and development*, Texas A&M University Press, College Station, Temple, TX.

Kaiser, E. A., K. Kohrs, M. Kucke, E. Schnug, O. Heinemeyer, and C. Munch (1998), Nitrous oxide release from arable soil: importance of N fertilization, crops and temporal variation, *Soil Biol. Biochem.*, *30*, 1553–1563.

King, D., J. Daroussin, and M. Jamagne (1994), Proposal for a spatial organization model in soil science (the example of the European Communities soil map), *J. Am. Soc. Inform. Sci.*, *45*, 705–717.

Li, C., Y. Zhuang, M. Cao, P. Crill, Z. Dai, S. Frolking, B. M. III, W. Salas, W. Song, and X. Wang (2001), Comparing a process-based agro-ecosystem model to the IPCC methodology for developing a national inventory of N2O emissions from arable lands in China, *Nutr. Cycl. Agroecos.*, *60*, 159–175.

Li, C. S., S. Frolking, X. M. Xiao, B. Moore, S. Boles, J. J. Qiu, Y. Huang, W. Salas, and R. Sass (2005), Modeling impacts of farming management alternatives on CO2, CH4, and N2O emissions: A case study for water management of rice agriculture of China, *Global Biogeochem. Cycles*, *19*, GB3010, doi:10.1029/2004GB002341.

Loyce, C., J. P. Rellier, and J. M. Meynard (2002), Management planning for winter wheat with multiple objectives (2): ethanol-wheat production, *Agric. Syst.*, *72*, 33–57.

Mosier, A. R., J. M. Duxbury, J. R. Freney, O. Heinemeyer, and K. Minami (1996), Nitrous oxide emissions from agricultural fields: Assessment, measurement and mitigation, *Plant Soil*, *181*, 95–108.

Mosier, A. R., C. Kroeze, C. Nevison, O. Oenema, S. Seitzinger, and O. V. Cleemput (1998), Closing the global $N_2O$ budget: nitrous oxide emissions through the agricultural nitrogen cycle, *Nutr. Cycl. Agroecos.*, *52*, 225–248.

Mummey, D. L., J. L. Smith, and G. Bluhm (1998), Assessment of alternative soil management practices on $N_2O$ emissions from US agriculture, *Agric. Ecosys. Environ.*, *70*, 79–97.

Parton, W. J., E. A. Holland, S. J. D. Grosso, M. D. Hartman, R. E. Martin, A. R. Mosier, D. S. Ojima, and D. S. Schimel (2001), General model for $NO_x$ and $N_2O$ emissions from soils, *J. Geophys. Res.*, *106*, 17,403–17,419.

Smith, J. U., P. Smith, and T. M. Addiscott (1996), Quantitative methods to evaluate and compare Soil Organic Matter (SOM) models, in *Evaluation of Soil Organic Matter Models*, edited by D. S. Powlson, J. U. Smith, and P. Smith, pp. 181–199, Springer-Verlag, Berlin Heidelberg.

Ulrich, E., and B. Willot (1993), Les dépôts atmosphériques en france de 1850 à 1990, *Synthèse*, A.D.E.M.E./O.N.F./I.N.R.A., Office National des Forêts, Paris.

Velthof, G. L., P. J. Kuikman, and O. Oenema (2003), Nitrous oxide emission from animal manures applied to soil under controlled conditions, *Biol. Fert. Soils*, *37*, 221–230.

Yanai, J., T. Sawamoto, T. Oe, K. Kusa, K. Yamakawa, K. Sakamoto, T. Naganawa, K. Inubushi, R. Hatano, and T. Kosaki (2003), Spatial variability of nitrous oxide emissions and their soil-related determining factors in an agricultural field, *J. Environ. Qual.*, *32*, 1965–1977.

Zheng, X., S. Han, Y. Huang, Y. Wang, and M. Wang (2004), Re-quantifying the emission factors based on field measurements and estimating the direct $N_2O$ emission from Chinese croplands, *Global Biogeochem. Cycles*, *18*(GB2018), doi: 10.1029/2003GB002167.

---

B. Gabrielle, INRA, INA P-G, UMR 1091 Environnement et Grandes Cultures, 78850 Thiverval-Grignon, France. (Benoit.Gabrielle@grignon.inra.fr)